

# Interfacial adsorption and denaturation of human milk and recombinant rice lactoferrin

Fang Pan, XiuBo Zhao, Thomas A. Waigh, and Jian R. Lu<sup>a)</sup>

*Biological Physics Group, Schuster Building, The University of Manchester, Oxford Road, Manchester M13 9PL, United Kingdom*

Fausto Miano

*S.I.F.I. S.p.A., Via Ercole Patti, 36-95020 Aci S. Antonio-Laviniaio (Catania), Italy*

(Received 20 May 2008; accepted 8 July 2008; published 29 August 2008)

Lactoferrin (LF) produced from recombinant technologies can achieve almost identical amino acid sequences and three-dimensional structures to those extracted from mammals, but differences often arise in the carbohydrate chains attached through *N*-glycosylation, with altered sizes, structures, and chemical nature. We compare the differences in solvation and interfacial adsorption from two samples, human milk lactoferrin (hLF) and recombinant rice lactoferrin (rLF). Lactoferrin is a bilobal protein with a molecular weight of about 80 kD. It has three *N*-glycosylation sites. Each of the three attached glycan chains on rLF contains seven to eight sugar groups. In comparison, each of the three glycan chains attached to hLF contains 12–13 sugar groups and is twice as long. The rLF melting point in 1 mg/ml aqueous solution (*pH* 7 phosphate buffer, *I*=20 mM) was 43 °C from dynamic light scattering, compared to 53 °C for hLF, exhibiting the enhanced solvation and stability of hLF due to its longer carbohydrate side chains. Silicon oxide surfaces provided a model substrate for assessment of lactoferrin adsorption and comparison with other proteins. The time dependent interfacial adsorption studied by spectroscopic ellipsometry (SE) was characterized by a fast initial step followed by a slow relaxation process. In addition, the SE results revealed the persistently higher adsorption of rLF, again showing the effect of glycan side chains. In spite of the different adsorbed amounts, neutron reflection revealed similar interfacial structures of the adsorbed protein layers. At the low lactoferrin concentration around 10 mg/l, a flat-on molecular monolayer formed with both LF lobes attached to the SiO<sub>2</sub> surface through electrostatic attraction. As the protein concentration increased, a secondary molecular layer further adsorbed to the first one and the attachment was again driven by electrostatic attraction. The intermixing between the globular lobes resulted in the dense packing in the middle 60 Å with some of the lobes projected toward the aqueous bulk solution. © 2008 American Vacuum Society. [DOI: 10.1116/1.2965135]

## I. INTRODUCTION

Lactoferrin (LF) is an important protein in tears. Together with several other proteins such as immunoglobulins, and lysozyme, they form the host defense system of the external eye.<sup>1,2</sup> LF is an iron complexing protein and exhibits both bacteriostatic and bactericidal properties.<sup>3,4</sup> LF has a strong inhibitory effect on complementary activations and inflammatory cascades.<sup>5–7</sup> In addition to the benefits to eye care and general health, adsorption of LF onto contact lenses may help protect the devices from bacterial infection. However, interaction between LF and contact lenses causes structural unfolding and the loss of biological activities, leading to adverse cascades of inflammatory processes and ocular diseases.<sup>8,9</sup> Given different biological and medical implications, it is important to study the surface and interfacial adsorption of LF under tear mimicking solutions.

LF also exists in the milk of most mammals and is a major protein component of secreted fluids such as saliva, gastric juice, bile, and other exocrine secretions of mam-

mals.<sup>3</sup> It works to protect surfaces such as teeth or tissue surfaces by forming thin protein films together with other proteins. The structure and composition of the film affects the subsequent colonization of microbes on the surface or interface concerned. In healthy native biological environments, LF protective functions are associated with its adsorption and binding to decrease the adherence and growth of hazardous microbes and sustain a healthy environment.<sup>10</sup> In this regard, LF bioactivities represent a novel therapeutic agent with a wide range of potentials. Recent studies have revealed that both whole LF proteins and their trypsin digested peptide products share similar antimicrobial and anti-inflammatory effects.<sup>11</sup>

The potentials offered by LF have stimulated the development of various recombinant technologies for an efficient and economical production of LF in anticipation of large biotechnological demands. Among the different expression systems, plants have been extensively explored. This is mainly because plants offer advantages such as product stability, easy storage, absence of pathogenic contaminants or other infectious agents for humans and animals, proper folding of the proteins with continued biological activity, and structural integrity.<sup>12</sup> Although most recombinant systems

<sup>a)</sup> Author to whom correspondence should be addressed; Tel.: 44-161-3063926; electronic mail: j.lu@manchester.ac.uk

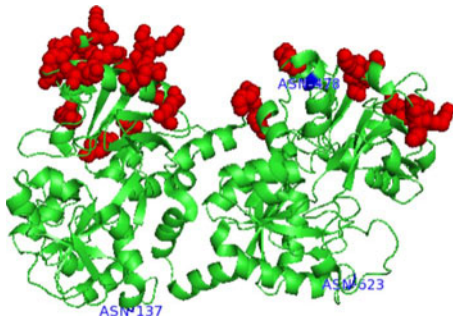


FIG. 1. Schematic representation of bilobal LF molecule. The space filled amino acids labeled in red represent the open regions carrying net positive charges on each lobe. The three Asn residues for *N*-glycosylation are marked in blue.

provide around 99% identical amino acid sequences for glycoproteins, differences occur in the glycan chains.<sup>13,14</sup> Glycosylation is important for the prevention of immunogenicity of the protein, its pharmacokinetic profile, solubility, and stability against proteolysis.<sup>15</sup>

LF contains some 700 amino acid residues with a molecular weight of ~80 000.<sup>16–18</sup> It has a bilobal and symmetrical structure. Each lobe contains one iron-binding site. Amino acid sequence alignments showed that there is some 40% sequence identity between its N- and C-terminal halves. Each lobe has a large outer surface area decorated with basic clusters of residues (labeled in red in Fig. 1) and is responsible for binding to anionic molecules such as lipopolysaccharide (LPS), heparin, or cell surface heparin sulfates. The three-dimensional (3D) crystalline structure of lactoferrin has been revealed by x-ray studies with different resolutions<sup>16–18</sup> and its bilobal contour shape is schematically shown in Fig. 1. The overall dimensions are approximately 152 × 95 × 56 Å<sup>3</sup>, with the approximate dimensions for each ellipsoidal lobe being 55 × 35 × 35 Å<sup>3</sup>. An  $\alpha$ -helical hinge links the two lobes and their long axes are roughly antiparallel. Our previous small angle neutron scattering (SANS) work has

already indicated that the  $\alpha$ -helical connection offers flexibility for orientational adjustment in aqueous solution in response to different electrostatic interactions.

As was already reported, glycosylation differs between plant and mammal derived LFs and the main glycan chain structures from recombinant rice LF (rLF) and human milk LF (hLF) are compared in Fig. 2.<sup>14</sup> The structural differences may affect solubility, stability, appropriate folding, and biological function. Lactoferrin contains three potential *N*-glycosylation sites located at Asn137 in the N lobe and Asn478 and Asn623 in the C lobe, and their relative locations on the bilobal structure are shown in Fig. 1.<sup>18,19</sup> In hLF, the two first *N*-glycosylation sites are substituted by complex-type *N*-glycans, whereas the third one (Asn623) is mostly unglycosylated.<sup>20</sup> The attached carbohydrate chains contain mammalian type of sugar residues such as  $\alpha$ 2-6-linked NeuAc and  $\beta$ 1-4 galactose at the nonreducing ends and  $\alpha$ 1-6-linked Fuc at the proximal glucosamine core of Man3GlcNAc2. In contrast, plant-specific structures contain  $\alpha$ 1-3-linked fucose and  $\beta$ 1-2-linked xylose and the glycan chains are overall shorter.

The aim of this work is to study how differences in sugar side chains affect their interfacial adsorption. As silicon oxide has been widely used as a model substrate to assess protein adsorption,<sup>21</sup> it has also been used in the current work to facilitate the comparison between human milk hLF and recombinant rice rLF. Silicon oxide surfaces bear weak negative charges and the charge density shows a slight increase with *pH* over *pH* 5. In contrast, LF has the isoelectric point (IEP) around 8.5 and is thus net positively charged below the IEP. The measurement of the density distribution of the interfacial layer provides a useful indication about what structural conformations the bilobal molecule adopts at the silicon oxide/water interface. Inhomogeneity in the length scale less than the shortest axial length is a strong indication of structural deformation or unfolding of the globular morphology. Our neutron reflection studies indicate the formation of a protein monolayer at low solution concentrations. However, as the bulk concentration increases further, adsorption occurs

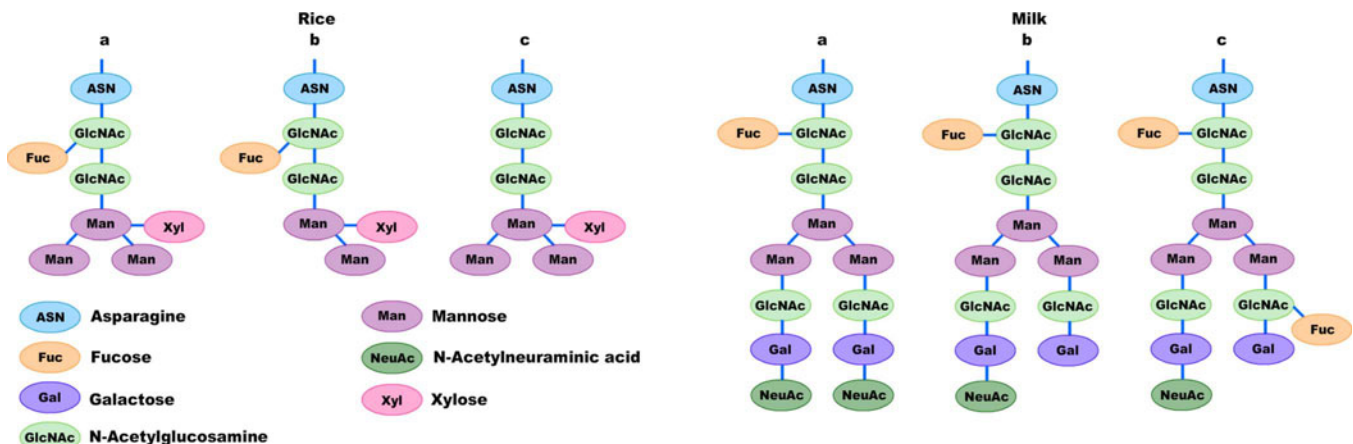


FIG. 2. Comparison of glycosylation patterns between rice rLF and hLF.

and the layer becomes rather disorganized, indicating strong structural flexibility, but there was no structural indication of unfolding of the lobes.

## II. EXPERIMENT

Neutron reflection experiments were performed at ISIS Neutron Facility, Rutherford Appleton Laboratory near Oxford, U.K., using reflectometer SURF. The reflectometer used a white neutron beam with wavelength from 0.5 to 6.5 Å. Measurements were made by clamping a perspex trough against the polished face of a silicon <111> block of dimensions of  $6 \times 5 \times 1.2$  cm<sup>3</sup> and the sample cell was filled with 2 ml of solution. The sample cell was mounted on a goniometer stage linked to a control computer terminal. The neutron beam entered the small face of the silicon block, reflected from the solid/solution interface, and exited from the opposite end of the block. The neutron beam was defined by two sets of horizontal and vertical slits placed before the sample cell, providing a typical beam illuminated area around  $4 \times 3$  cm<sup>2</sup>. Each reflectivity scan was carried out at three incidence angles of 0.35°, 0.8° and 1.8° and the resulting reflectivity profiles combined to cover wave vectors ( $k$ ) between 0.012 and 0.5 Å<sup>-1</sup>. Reflectivity profiles below the critical angle were theoretically equal to unity and all the data measured were scaled accordingly. Constant backgrounds were subtracted using the average reflectivity between 0.25 and 0.5 Å<sup>-1</sup>. The background were typically found to be around  $2 \times 10^{-6}$  in D<sub>2</sub>O.

Protein unfolding temperatures ( $T_m$ ) were determined using the Zetasizer Nano-S (model ZEN1600) instrument from Malvern Instruments Ltd. This instrument can measure particle sizes in the range of 0.6 nm–6 μm, over a wide range of concentrations (0.1 mg/ml to 40% w/v) and at temperatures from 2 to 90 °C. In this work, the two protein solutions [1 mg/ml in phosphate buffer in H<sub>2</sub>O at pH 7 and a total ionic strength ( $I$ ) of 20 mM] were measured as a function of temperature from 25 to 65 °C inside a quartz cell.

Spectroscopic ellipsometry (SE) measurements were made using a Jobin–Yvon UVISEL SE over a typical wavelength range of 300–600 nm. A liquid cell was specially constructed for the SE measurements at the solid/liquid interface with the incident light at 70° with respect to the sample surface. The experimental data were analyzed to give the thickness ( $\tau$ ) and the refractive index ( $n$ ) of the layer using the DELTAPSI2 software developed by Jobin–Yvon. The amount of protein adsorbed was calculated using the equation proposed by de Feitjer *et al.*:

$$\Gamma = \frac{\tau(n - n_w)}{a}, \quad (1)$$

where  $n_w$  is the refractive index of the aqueous phase;  $a$  indicates the change in the refractive index of the protein solution with increasing concentration,<sup>22</sup> and its value is close to 0.18 cm<sup>3</sup>/g for a variety of different globular proteins.

Human milk lactoferrin purchased from Sigma with a molecular weight of about 80 kD was used as supplied. The

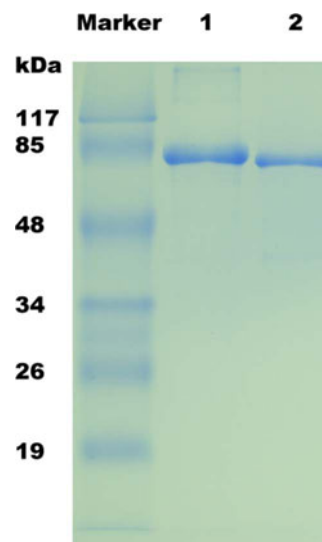


FIG. 3. SDS-PAGE of marker (1 μg/protein), hLF (1) and rLF (2) (2 μg/lane).

protein contained some 30% iron ions equivalent to the binding sites available. Lactoferrin from rice was supplied by Ventria Bioscience. This derived recombinant lactoferrin has a molecular weight of 78.5 kD and a purity higher than 90% (SDS PAGE). Further details on lactoferrin from rice are published in Ref. 23. The D<sub>2</sub>O used was purchased from Sigma with a deuterium content of 99.9%. The surface tension of the D<sub>2</sub>O at ambient temperatures was found to be close to 70 mN/m using a Kruss K11 tensiometer. Ultrapure water (Ulgastat ultrapure, ultrahigh quality) was used for washing and rinsing of the glassware and trough. The NaCl used was analytical reagent (AR) grade from Sigma–Aldrich. Phosphate buffers in H<sub>2</sub>O and D<sub>2</sub>O with a total ionic strength of 20 mM were made to hold the solutions at pH 7.

12% tris-glycine SDS-PAGE experiment was performed using the Bio-Rad Mini-Protein® 3 cell and following the instruction manual. 5 μl (1 μg/protein) of prestained protein molecular weight marker (SM0441, Fermentas, UK) was used as the molecular marker. The two lactoferrin proteins were loaded at 2 μg/well. The experiment was carried out at 120 V for 1 h, after which the gel was stained by coomassie brilliant blue G-250 (Fisher, UK) for 30 min followed by destaining overnight. The images were recorded using a SONY DSC T100 digital camera. All the measurements were made at the ambient temperature of 22–23 °C.

## III. RESULTS AND DISCUSSION

To check the purities of the two LF samples, we used SDS-PAGE protein gel electrophoresis. The results shown in Fig. 3 reveal very high purities for both types of sample. Comparison to the reference protein markers indicates that the molecular weight for hLF is about 80 000 and that for rLF is slightly lower. The difference arises from the smaller glycan chains attached to rLF.<sup>23,24</sup> The glycan chain structures of rLF derived from rice and hLF from human milk have been extensively studied,<sup>14</sup> and the structures shown in

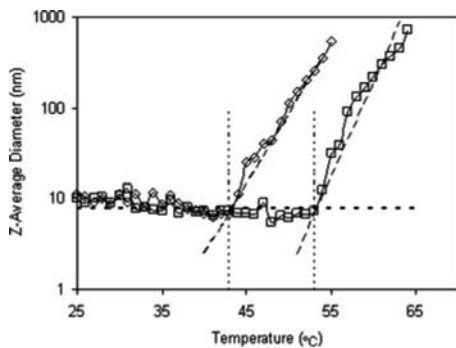
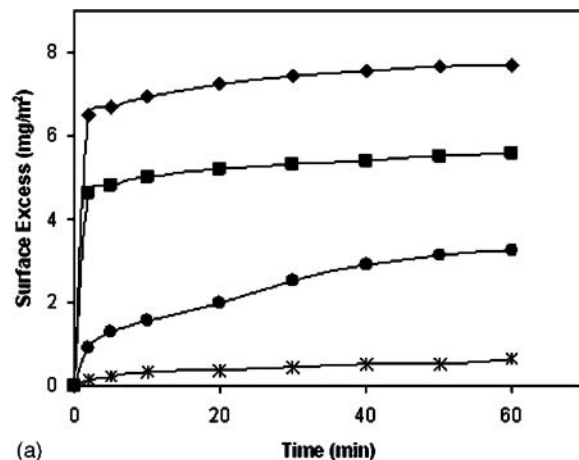


Fig. 4. Unfolding transition of rLF (43 °C) and hLF (53 °C) (1 mg/ml, phosphate buffer pH 7,  $I=20$  mM).

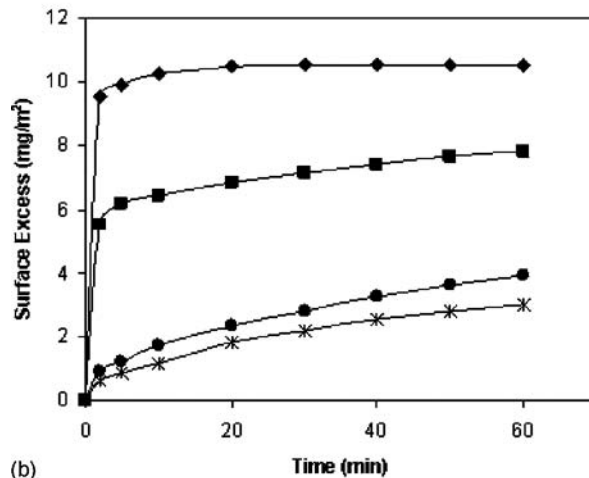
Fig. 2 are from the recent work of Fujiyama *et al.*<sup>14</sup> The main glycans in rice rLF are group (a) (M3FX, 42.5%) and group (b) (M2FX, 39.1%), while group (c) occupies a smaller fraction (6%). N-linked oligosaccharides in plants have  $\beta$ 1-2-xylose and  $\alpha$ 1-3-fucose residues and lack galactose and *N*-acetylneuraminic acids (NeuAcs, sialic acid), as identified from milk hLF, consistent with plant post-translational modification patterns.<sup>14</sup> In addition to the different structures and compositions, the overall glycan size from hLF is greater and is consistent with the larger molecular weight displayed in the SDS-PAGE plate in Fig. 3.

The attachment of different N-linked glycan structures has different implications for the solvation and stability of LF molecules. Altered carbohydrate groups interact differently through hydration with the solvent. The strength of the hydration can be assessed by heating the protein solution while monitoring the occurrence of aggregation using dynamic light scattering (DLS).<sup>25</sup> Figure 4 shows the number averaged ( $z$ -average) diameter of LF based on the intensity of scattered light. The protein unfolding transition  $T_m$  is the temperature at which the heating causes the opening up of the protein molecules. The increase in the apparent size detected indicates the start of aggregation, signifying protein denaturation. Figure 4 shows that over the low temperature range, increase in temperature leads to a small but measurable decrease in LF diameter from 12 nm at 25 °C to 8 nm at 40 °C. This steady decrease reflects the possible dehydration without any major structural disruption to both hLF and rLF. However, a sharp increase in size is detected at 43 °C for rLF and at 53 °C for hLF, indicating the onset of aggregation. Given that the primary amino acid sequences and 3D structures are almost identical, the difference observed is consistent with the different sizes of N-linked glycan structures attached to the two LFs. Any effects relating to glycan structures may also affect their functions when glycoproteins are used as pharmaceuticals or as ingredients for nutrient formulations. Changes in size associated with protein denaturation can be easily identified using DLS.

SE can undertake an adsorption measurement over the time scale of 1 min (Ref. 26) and has been used to study the time dependent adsorption of LF at the hydrophilic silicon oxide/water interface. The measurements were made at the ambient temperature of 22–23 °C and the solution pH was



(a)



(b)

Fig. 5. Adsorption of (a) hLF and (b) rLF at the hydrophilic silicon oxide/water interface at 0.002 (\*), 0.01 (●), 0.1 (■), and 1 (◆) mg/ml in pH 7 phosphate buffer with  $I=20$  mM. The lines were drawn to guide the eye.

controlled at pH 7 using phosphate buffer, with the total ionic strength ( $I$ ) fixed at 20 mM. For each LF, the measurements were made at four representative concentrations and the results shown in Fig. 5 indicate a similar trend of increase in the surface adsorbed amount (surface excess  $\Gamma$ ) with LF concentration. The adsorption profiles from both LFs at high concentrations show a characteristic two step process: a fast initial adsorption over the first 2–3 min followed by a slow adsorption process indicating structural relaxation and rearrangement. This feature is very similar to the general pattern observed from peptides and polyelectrolytes and is very different from globular proteins such as IgGs, indicating that the LFs have great structural flexibility. On the other hand, the adsorption profiles from both LFs at low concentrations increased steadily.

The surface excesses obtained from rLF are consistently higher than those from hLF over the entire concentrations studied. The increased number of *N*-acetylneuraminic acids (sialic acids) bound to hLF presents a sizable electrostatic barrier to adsorption (negative carbohydrate groups repelled from negative silicon oxide). Furthermore, the increased size in the carbohydrate side chains in hLF will tend to decrease adsorption due to their increased entropic steric effect.

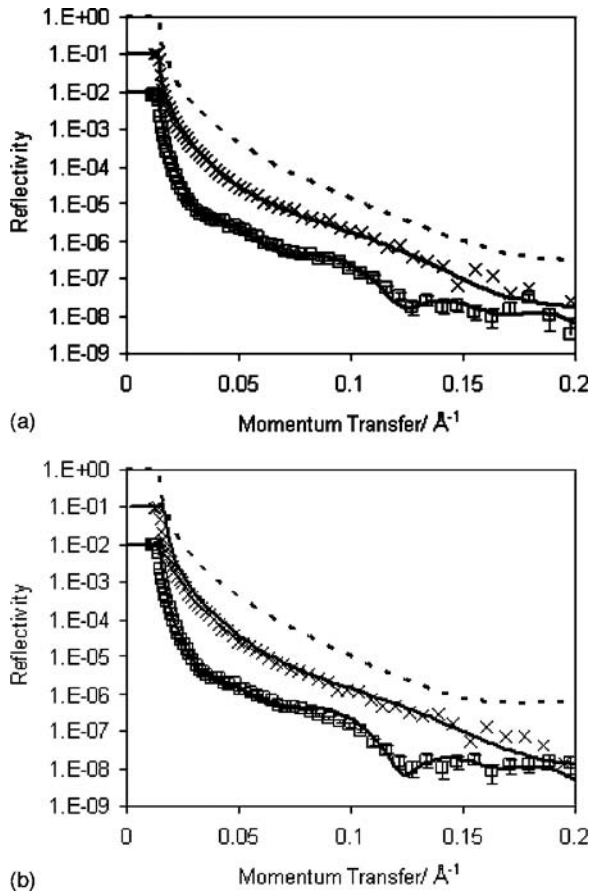


FIG. 6. Neutron reflectivity profiles measured from adsorption of (a) hLF and (b) rLF at 10 mg/l ( $\times$ , offset one magnitude along the vertical axis for clarity) and 100 mg/l rLF ( $\square$ , offset two magnitudes along the vertical axis for clarity) in pH 7 phosphate  $D_2O$  buffer with  $I=20$  mM at the silicon oxide/solution interface. The continuous lines represent the best fits with structural parameters listed in Table I. The reflectivity measured from the  $D_2O$  buffer is shown as the dashed line for comparison.

Neutron reflection (NR) has been extensively used to determine the thickness and composition of protein layers,<sup>21</sup> revealing the structural packing of the molecules at surfaces. As it took about 1 h to complete each NR measurement, NR data represent the average layer structure under given solution conditions. Each measurement started after a 1 h equilibration period to avoid time dependent adsorption, as revealed from the SE studies. To provide increased scattering length density contrast for the adsorbed protein layers, all NR solutions were prepared in  $D_2O$  instead of  $H_2O$ . Prior to the protein adsorption study, the bare silicon oxide surface was characterized with a NR measurement of the silicon oxide/pure  $D_2O$  interface. The native oxide layer was found to be  $13 \pm 2$  Å, with the scattering length density ( $\rho$ ) equal to  $3.4 \times 10^{-6}$  Å<sup>-2</sup>. The value of  $\rho$  is the same as that for the native  $SiO_2$ , which indicates a smooth oxide surface without any penetration of the  $D_2O$ . The mixing of  $D_2O$  would indicate the presence of defects over the interface.

The reflectivity profiles measured for LF adsorption under two representative concentrations are shown in Fig. 6(a) for hLF and in Fig. 6(b) for rLF. Adsorption of LF onto the bare

silicon oxide leads to changes in the reflectivity compared to that measured in pure  $D_2O$ . As the concentration of LF increases, the extent of the deviation intensifies.

The measured reflectivity profiles were analyzed using an optical matrix formula.<sup>27,28</sup> A uniform layer model was first applied to fit the protein layer formed on the smooth  $SiO_2$  surface with the structure for the oxide layer fixed. The thickness ( $\tau$ ) and layer scattering length density ( $\rho$ ) were varied to obtain a good fit. Changes in  $\tau$  and  $\rho$  had different effects on the resultant reflectivity profiles;  $\tau$  affected the shape and  $\rho$  affected the absolute level. The results show that at low concentrations of 10 mg/l, the adsorption led to the formation of a protein layer of  $47 \pm 4$  Å, with a layer scattering length density of  $5.9 \times 10^{-6}$  Å<sup>-2</sup>. Figure 6 shows that the calculated curve reproduces the measured one, indicating that under these conditions the distribution of the protein fragments within the layer can be well represented by this simple model. The protein layer is fully immersed in water, so the relationship between  $\tau$  and  $\rho$  can be described through the following equation:

$$\rho = \frac{b_p + n_w b_w}{A\tau}, \quad (2)$$

where  $b_p$  is the scattering length of the protein in  $D_2O$ ,  $n_w$  is the number of water associated with the protein, and  $b_w$  is its scattering length. The number of water molecules in the layer should satisfy the volume restriction requirement

$$A\tau = V_p + n_w V_w. \quad (3)$$

$V_p$  and  $V_w$  are the respective volumes of protein and water molecules and  $A$  is the area per molecule and is related to surface excess through

$$\Gamma = \frac{MW}{6.02A}, \quad (4)$$

where MW is the protein's molecular weight. The scattering length density of the layer can be calculated from

$$\rho = \phi_w \rho_w + \phi_p \rho_p,$$

where  $\rho_p$  and  $\rho_w$  represent the scattering length densities of protein and water and  $\phi_p$  and  $\phi_w$  are the respective volume fractions ( $\phi_p + \phi_w = 1$ ). From  $\tau$  and  $\rho$  obtained from the fitting,  $\phi_p$  was found to be 0.13 and  $\Gamma$  to be 0.9 mg/m<sup>2</sup>, indicating a low surface adsorption under this concentration.

At higher concentrations of 100 mg/l, a uniform layer model was found to be inappropriate to fit the measured reflectivity profile. A two layer model, consisting of a dense inner layer on the oxide surface and a loose outer layer into the aqueous solution, improved the fit. The best fit was produced when a three layer model was deployed that took into account an extra sublayer that has very little protein fragments in a narrow region close to the oxide surface. The structural parameters obtained for both hLF and rLF are listed in Table I, where it can be seen that the adsorption of both proteins again produces almost identical interfacial structures at high concentrations of 100 mg/l.

TABLE I. Structural parameters obtained from model fitting to both hLF and rLF adsorbed at the hydrophilic SiO<sub>2</sub>/D<sub>2</sub>O interface at the protein concentrations of 10 and 100 mg/l in pH 7 phosphate buffer with  $I=20$  mM. The SiO<sub>2</sub> layer was found to be  $13 \pm 2$  Å.

	$\tau$ (Å)	$\rho$ ( $10^{-6}$ Å <sup>-2</sup> )	$\phi$	$\Gamma$ (mg/m <sup>2</sup> )
10 mg/l hLF	47 ± 4	5.9	0.13	0.9 ± 0.2
10 mg/l rLF	47 ± 4	5.9	0.13	0.9 ± 0.2
100 mg/l hLF	6 ± 2	5.8	0.18	5.2 ± 0.3
	60 ± 3	5.1	0.42	
	60 ± 4	5.8	0.18	
100 mg/l rLF	6 ± 2	5.5	0.28	6.1 ± 0.3
	60 ± 3	4.8	0.52	
	60 ± 4	5.8	0.18	

The surface excesses obtained from SE and NR show a consistent trend of increasing adsorption with LF concentration. The results from NR show that the surface excesses from hLF and rLF are small at low concentrations around 10 mg/l. As the concentration is around 100 mg/l, rLF adsorbs more. As the difference between rLF and hLF is revealed from both SE and NR measurements the results again reflect the effect of different glycan side chains. It should be noted that the surface excesses from NR are consistently lower than those obtained from SE, but the differences are mostly within the experimental error range. The difference may arise from slightly different surface properties between silicon wafers and the large silicon blocks. The surface contact angles were all below 20°, but a slight difference in charge density might cause the apparent deviations.

At 10 mg/l, the area per molecule is  $14\,800$  Å<sup>2</sup> as compared to the surface area of  $14\,400$  Å<sup>2</sup> from the protein 3D crystalline structure. The close agreement suggests that there is sufficient surface area for the LF molecule to adsorb flat on the surface with one of its large faces in direct contact with SiO<sub>2</sub>. This proposition is consistent with the layer thickness of 47 Å, close to the short axial length of 56 Å. Further increases in bulk LF concentration will increase the lateral packing, but a progressive formation of a second protein layer mixed with the first one is evident from the NR measurements. The NR data analysis reveals that while the overall layer thickness increases, the attachment of the second layer onto the first layer resulted in the need of a three layer model to account for the inhomogeneous packing density along the surface normal direction.

The structural conformations of LF molecules adsorbed at the SiO<sub>2</sub>/water interface can be schematically shown in Fig. 7. At the low LF concentration of 10 mg/l, LF adsorption forms a flat-on molecular monolayer, with their short axial length projected perpendicular to the SiO<sub>2</sub> surface. The space filled amino acid residues marked in red in Fig. 1 on each lobe represents the surface region that bears net positive charges that are easily accessible. Because the two globular lobes are linked through an  $\alpha$ -helical hinge, it must be rather flexible for the two lobes to adjust their contacts with the SiO<sub>2</sub> surface. As the LF concentration increases, the monolayer becomes fully packed. As LF surfaces bear uneven

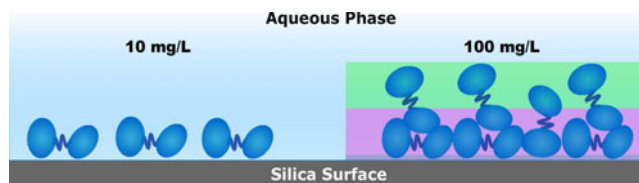
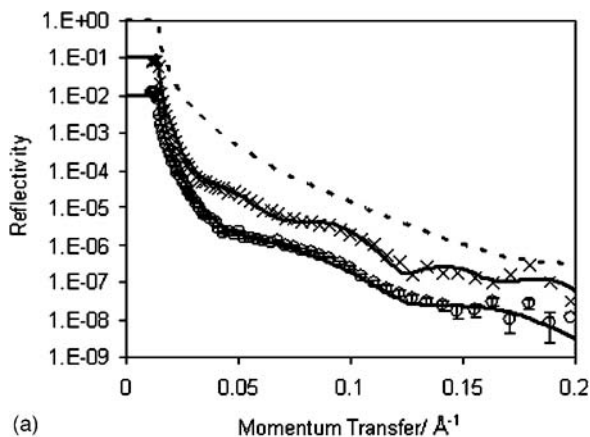


FIG. 7. Schematic representation of the structure of LF layers formed at 10 mg/l (left) and 100 mg/l (right) at the hydrophilic silicon oxide/water interface.

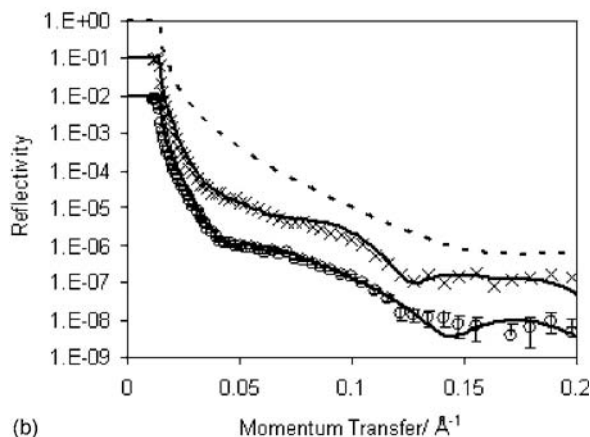
charges and hydrophobic distributions, a less dense secondary layer forms on top of the first one. The intermixing of the two molecular monolayers results in the high packing density in the middle of the film. The interactions within the interfacial regions may cause further structural readjustments. This is evident in the occurrence of a 5 Å sublayer with less protein nearest the SiO<sub>2</sub> surface. Thus, in terms of polypeptide density distribution, the molecular bilayer can be modeled using a three layer model, as previously described, the middle sublayer of some 60 Å consisting of the main body of LF, the outer sublayer of some 60 Å containing LF lobes loosely projected into the aqueous solution, and the inner sublayer of some 5 Å with less protein fragments due to structural constraints and possible electrostatic repulsion. This analysis indicates that the bilobal proteins retain their globular structures and the  $\alpha$ -helical hinge offers flexibility as well as confinement. This is in contrast with mucin MUC6 glycoproteins, where the globular dumbbells form flat pancakes on SiO<sub>2</sub> surfaces in atomic force microscopy measurements.<sup>29</sup>

The effect of ionic strength on LF adsorption has been examined by increasing the concentration of NaCl. As the isoelectric point for LF is around 8.5, the protein is net positively charged at pH 7 and the interfacial adsorption is driven by the electrostatic attraction with the negatively charged SiO<sub>2</sub> surface. An increase in ionic strength screens the electrostatic force and leads to the decrease in surface adsorption. Figure 8 shows a comparison of neutron reflectivity profiles measured from 100 mg/l hLF [Fig. 8(a)] and rLF [Fig. 8(b)] with and without 0.15 NaCl (see Table II). The addition of salt reduces LF adsorption, an observation consistent with the trend obtained from other globular proteins such as lysozyme and human serum albumin.<sup>23,30–33</sup> The reduced adsorption is evident from the shift in the broad interference fringes to the higher wave vectors, showing the dominant effect of electrostatic interaction in regulating intermolecular forces at the interface. Data analysis revealed a structural model similar to that obtained without the addition of NaCl, but the amount of the LF adsorbed in the outer sublayer was substantially reduced. Because of the low LF content in the outer sublayer, we were unable to determine the precise thickness from the NR data analysis.

The effect of the total ionic strength on surface excess is plotted in Fig. 9. While both LFs show a decreasing trend of surface excess with increasing ionic strength, the responses from the two proteins are different. It can be seen from Fig. 9 that above 0.06 mM the adsorption of rLF does not re-



(a)



(b)

Fig. 8. Neutron reflectivity profiles measured at 100 mg/l hLF (a) and 100 mg/l rLF (b) in pH 7 D<sub>2</sub>O phosphate buffer ( $I=20$  mM) with (○, offset two magnitudes along the vertical axis for clarity) and without (×, offset one magnitude along the vertical axis for clarity) 0.15M NaCl. The continuous lines represent the best fits with structural parameters listed in Table II. The reflectivity measured from the D<sub>2</sub>O buffer is shown as the dashed line for comparison.

spond to the further increase in ionic strength, while a decrease in surface excess with the increase in ionic strength is displayed for hLF. The different responses can also be attributed to the different glycan side chains. Figure 2 shows that as well as the different sizes and structures of the sugar side chains, most of the terminal glycan groups on hLF are neuraminic acids, which are weak negatively charged. These glycan side chains appear to facilitate more effective repul-

TABLE II. Structural parameters obtained from model fitting to both hLF and rLF adsorbed at the hydrophilic SiO<sub>2</sub>/D<sub>2</sub>O interface at the protein concentration of 100 mg/l in pH 7 phosphate buffer with  $I=20$  mM and with addition of 0.15M NaCl. The SiO<sub>2</sub> layer was found to be  $13 \pm 2$  Å.

	$\tau$ (Å)	$\rho$ ( $10^{-6}$ Å <sup>-2</sup> )	$\phi$ (%)	$\Gamma$ (mg/m <sup>2</sup> )
100 mg/l hLF, 0.15M NaCl	6	6	11.7	2.63
	60	5.5	28.4	
	10	6	11.7	
100 mg/l rLF	4	5.5	28.2	4.0
0.15M NaCl	60	5.1	42.1	
	30	6.1	8.1	

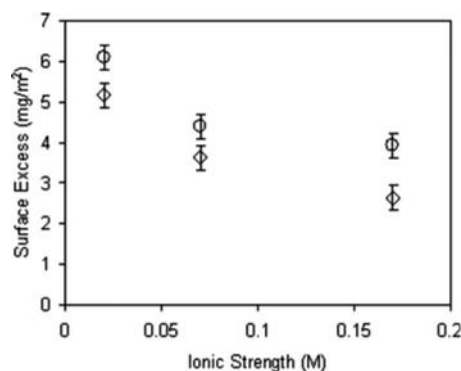


Fig. 9. Surface excess of hLF (◇) and rLF (○) plotted against the total ionic strength.

sions with the SiO<sub>2</sub> and between the adsorbed hLF layer, causing a steady decline in the amount of surface adsorbed proteins.

#### IV. CONCLUSIONS

Lactoferrin is an important protein with applications in food additives and pharmaceutical formulations. With its increasing demand, various biotechnologies have been developed to produce this protein in recombinant forms. Its harvesting from rice offers an attractive production route, but plants express different *N*-glycosylated side chains from those obtained from mammals. Different glycosylated side chains can affect the solubility and interfacial binding properties of the glycoprotein, resulting in different pharmaceutical behaviors. We have examined the physiochemical properties connected with the different glycosylation patterns from rice and human lactoferrins.

hLF exhibits better hydration and solubility in aqueous solution than rLF. The difference is reflected in the unfolding temperatures ( $T_m$ ) measured with DLS. Different glycan chain sizes and structures also affect the amount of LF adsorption on the SiO<sub>2</sub> surface. The comparative study of changes in adsorption with increasing ionic strength reveals the possible effect of the terminal carboxyl groups from hLF.

Although there are different adsorbed amounts and different extents of solvation, the basic structures of the rLF and hLF protein layers are similar. At low LF concentrations, both proteins form a flat-on monolayer with both of their lobes in direct contact with the weak negatively charged SiO<sub>2</sub> surface. As N and C lobes have a large positively charged area on their outer surfaces, these surface regions are likely to be in direct contact with the substrate. At higher concentrations of 100 mg/l, a LF molecular bilayer forms. LF molecules adsorbed in the outer layer have one of their lobes intermixed with the outer region of the first monolayer. As a result, the majority of LF lobes are distributed in the middle part of the interface, and the LF lobes projected toward the outer surface are relatively low in their packing density.

## ACKNOWLEDGMENTS

The authors thank the Engineering and Physical Sciences Research Council (EPSRC) for support and the ISIS Neutron Facility at Rutherford Appleton Laboratory for provision of neutron beam time. One of the authors (F.P.) thanks the School of Physics and Astronomy, University of Manchester for studentship.

- <sup>1</sup>D. R. Korb, J. Craig, M. Doughty, J. P. Guillon, G. Smith, and A. Tomlinson, *The Tear Film: Structure, Function and Clinical Examination* (Butterworth & Heinemann, London, 2002)
- <sup>2</sup>A. F. Gachon and E. Lacazette, *Br. J. Ophthalmol.* **82**, 453 (1998).
- <sup>3</sup>J. H. Nuijens, P. H. C. van Berkel, and F. L. Schanbacher, *J. Mammary Gland Biol. Neoplasia* **1**, 285 (1996).
- <sup>4</sup>B. Reiter, J. H. Brock, and E. D. Steel, *Immunology* **28**, 83 (1975).
- <sup>5</sup>R. T. Ellison III, T. J. Giehl, and F. F. La, *Infect. Immun.* **56**, 2774 (1988).
- <sup>6</sup>L. Sanchez, M. Calvo, and J. H. Brock, *Arch. Dis. Child* **67**, 657 (1992).
- <sup>7</sup>J. R. Zucali, H. E. Broxmeyer, D. Levy, and C. Morse, *Blood* **74**, 1531 (1989).
- <sup>8</sup>M. C. Wahlgren, T. Arnebrant, and M. A. Paulsson, *J. Colloid Interface Sci.* **158**, 46 (1993).
- <sup>9</sup>Q. L. Luo and J. D. Andrade, *J. Colloid Interface Sci.* **200**, 104 (1998).
- <sup>10</sup>B. J. Appelmek, Y. Q. An, M. Geerts, B. G. Thijs, H. A. de Boer, D. M. MacLaren, J. de Graaff, and J. H. Nuijens, *Infect. Immun.* **62**, 2628 (1994).
- <sup>11</sup>H. A. van Veen, E. J. Geerts, P. H. C. van Berkel, and J. H. Nuijens, *Eur. J. Biochem.* **271**, 678 (2004).
- <sup>12</sup>H. Daniell, S. J. Streatfield, and K. Wycoff, *Trends Plant Sci.* **6**, 219 (2001).
- <sup>13</sup>T. Liu, Y. Zhang, and X. Wu, *J. Biotechnol.* **118**, 246 (2005).
- <sup>14</sup>K. Fujiyama, Y. Sakai, R. Misaki, I. Yanagihara, T. Honda, H. Anzai, and T. Seki, *Biosci., Biotechnol., Biochem.* **68**, 2565 (2005).
- <sup>15</sup>N. Jenkins and E. M. Curling, *Enzyme Microb. Technol.* **16**, 354 (1994).
- <sup>16</sup>B. F. Anderson, H. M. Baker, E. J. Dodson, G. E. Norris, S. V. Rumball, J. M. Waters, and E. N. Baker, *Proc. Natl. Acad. Sci. U.S.A.* **84**, 1769 (1987).
- <sup>17</sup>N. A. Peterson, V. L. Arcus, B. F. Anderson, J. W. Tweedie, G. B. Jameson, and E. N. Baker, *Biochemistry* **41**, 14167 (2002).
- <sup>18</sup>H. M. Baker, B. F. Anderson, and E. N. Baker, *Proc. Natl. Acad. Sci. U.S.A.* **100**, 3579 (2003).
- <sup>19</sup>H. M. Baker, C. J. Baker, C. A. Smith, and E. N. Baker, *JBIC, J. Biol. Inorg. Chem.* **5**, 692 (2000).
- <sup>20</sup>P. H. van Berkel, H. A. van Veen, M. E. Geerts, H. A. de Boer, and J. H. Nuijens, *Biochem. J.* **319**, 117 (1996).
- <sup>21</sup>J. R. Lu, X. Zhao, and M. Yaseen, *Curr. Opin. Colloid Interface Sci.* **12**, 9 (2007).
- <sup>22</sup>J. A. de Feijter, J. benjamins, and F. A. Veer, *Biopolymers* **17**, 1759 (1978).
- <sup>23</sup>S. Nandi, Y. A. Suzuki, J. Huang, D. Yalda, P. Pham, L. Wu, G. Bartley, N. Huang, and B. Lönnerdal, *Trends Plant Sci.* **163**, 713 (2002).
- <sup>24</sup>D. Rachmawati, T. Mori, T. Hosaka, F. Takaiwa, E. Inoue, and H. Anzai, *Breed. Sci.* **55**, 213 (2005).
- <sup>25</sup>See <http://www.azonano.com/details.asp?ArticleID=1224>.
- <sup>26</sup>E. Murphy, J. L. Kiddie, J. R. Lu, J. Brewer, and J. Russell, *Biomaterials* **20**, 1501 (1999).
- <sup>27</sup>J. R. Lu, E. M. Lee, and R. K. Thomas, *Acta Crystallogr., Sect. A: Found. Crystallogr.* **A52**, 11 (1996).
- <sup>28</sup>J. R. Lu and R. K. Thomas, *J. Chem. Soc., Faraday Trans.* **94**, 995 (1998).
- <sup>29</sup>G. Yakubov, A. Papagiannopoulos, E. Rat, and T. A. Waigh, *Biomacromolecules* **8**, 3791 (2007).
- <sup>30</sup>T. J. Su, J. R. Lu, R. K. Thomas, Z. F. Cui, and J. Penfold, *Langmuir* **14**, 438 (1998).
- <sup>31</sup>J. R. Lu, T. J. Su, R. K. Thomas, A. R. Rennie, and R. Cubit, *J. Colloid Interface Sci.* **206**, 212 (1998).
- <sup>32</sup>T. J. Su, J. R. Lu, R. K. Thomas, Z. F. Cui, and J. Penfold, *J. Phys. Chem. B* **102**, 8100 (1998).
- <sup>33</sup>T. J. Su, J. R. Lu, R. K. Thomas, and Z. F. Cui, *J. Phys. Chem. B* **103**, 3727 (1999).